Elyas Nurgat

Martin Berzins

School of Computer Studies,
University of Leeds,
Leeds, LS2 9JT, United Kingdom

Laurence Scales
Shell Research and Technology
Centre at Thornton,
Chester, CH1 3SH, United Kingdom

Solving EHL Problems Using Iterative, Multigrid, and Homotopy Methods

The numerical solution of ElastoHydrodynamic Lubrication (EHL) point contact problems requires the solution of highly nonlinear systems of equations which pose a formidable computational challenge. Multigrid methods provide one efficient approach. EHL problems solved using a single grid and multigrid will be compared and contrasted with a homotopy method which works on the concept of deforming one problem into another by the continuous variation of a single parameter. Both the multigrid and the single grid method employ a new relaxation scheme. Numerical results on demanding test problems will be used to compare these methods and suggestions for future developments to produce robust solvers will be made.

1 Introduction

This paper is concerned with a major computational difficulty that arises in the numerical solution of ElastoHydrodynamic Lubrication (EHL) (Gohar, 1988) problems, namely that of ensuring convergence of the nonlinear equations solver to a steady-state solution. Two successful methods which have been used for achieving this are direct iteration (e.g., Gauss Seidel) and multigrid methods.

Direct iteration methods have long been used (e.g. Hamrock and Dowson, 1977a) in conjunction with finite difference discretizations on regular meshes. Multigrid methods have also been used with great success by Venner (1994a) and Venner and Lubrecht (1994) with a good summary being given by Venner (1991b). These numerical methods have attractive properties such as rapid rate of convergence and are often used to solve the governing equations simultaneously. However, these numerical methods are not globally convergent in the sense that they can always locate a root from an arbitrary starting point. A fundamental limitation of these two methods is that it is not always possible to take a step that will guarantee a decrease in the residuals. In contrast, the relatively recently developed homotopy methods (Garcia, 1981) and (Allgower, 1990) are very powerful globally convergent methods but have a correspondingly greater computational cost.

These three approaches appear to provide efficient and reliable ways of solving EHL problems, but it is important to understand their relative merits and convergence criteria. This paper is a first attempt at providing such an understanding in the context of EHL point contact problems (contact of two spheres).

The layout of the remainder of this paper is as follows. In Section 2 we introduce the form of the equations to be solved. Multigrid method is described in Section 3 while Section 4 describes the new relaxation scheme and Section 5 describes the homotopy method. Sections 6 and 7 describe the test problems to be used in the comparison between the three methods and compare the performance of the three methods. Section 8 concludes the paper with a discussion of the merits of the three methods and suggests some future research directions.

2 Governing Equations

The mathematical model describing the isothermal EHL circular contact problem with oil entrainment in the positive X-direction consists of three nondimensional equations. The Reynolds equation relates pressure (P) to the film thickness (H) for a lubricant characterised by a pressure dependent viscosity η and density ρ

$$L(P) = \frac{\partial}{\partial X}\left(\epsilon \frac{\partial P}{\partial X}\right) + \frac{\partial}{\partial Y}\left(\epsilon \frac{\partial P}{\partial Y}\right) - \frac{\partial(\rho H)}{\partial X} = 0,\ X, Y \in [X_a, X_b] \times [Y_a, Y_b] \quad (1)$$

with the cavitation condition $P \geq 0$ and the boundary condition $P = 0$. The nondimensionalization is expressed in terms of the so-called Moes parameters L and M (Lubrecht et al., 1987a). Pressure is in units of the maximum Hertzian pressure

$$p_h = \frac{L}{\alpha\pi}\sqrt[3]{\frac{3M}{2}} \quad (2)$$

where α is the pressure coefficient of viscosity of the lubricant. X and Y are in units of Hertzian radius (b). Film thickness is in units of b^2/R, where R is the reduced radius of the contact. ϵ is given by

$$\epsilon = \frac{\rho H^3}{\eta\lambda} \quad (3)$$

where $\rho = 1 + (\mu p_h P/1 + \upsilon p_h P)$ if $P > 0$, otherwise $\rho = 1$ ($\mu = 5.8 \times 10^{-10}$ and $\upsilon = 1.68 \times 10^{-9}$ (Dowson and Higginson, 1977), $\eta = \exp\{(\alpha p_0/z)[-1 + (1 + (p_h/p_0)P)^z]\}$, ($p_0 = 1.98 \times 10^8$, and $z = 0.68$, (Roelands, 1966) and $\lambda = (4\pi/M)\sqrt[3]{(2/3M)}$.

The Film Thickness Equation, $H(X, Y)$, computes the elastic distortion of the surfaces caused by the pressure in the film and is written as:

$$H(X, Y) = H_0 + \frac{X^2}{2} + \frac{Y^2}{2} + \frac{2}{\pi^2}\int_{Y_a}^{Y_b}\int_{X_a}^{X_b} \frac{\dot{P}(X', Y')dX'dY'}{\sqrt{(X - X')^2 + (Y - Y')^2}} \quad (4)$$

where H_0 is a constant.

The final equation is the Force Balance Equation which ensures that the integral over the pressure balances the external applied load:

Contributed by the Tribology Division for publication in the JOURNAL OF TRIBOLOGY. Manuscript received by the Tribology Division February 3, 1997; revised manuscript received April 20, 1998. Associate Technical Editor: S. Ioannides.

$$\int_{Y_a}^{Y_b}\int_{X_a}^{X_b} P(X, Y)dXdY = \frac{2\pi}{3}. \quad (5)$$

2.1 Finite Difference Discretization of Governing Equations. The focus of this study is on the iterative solution methods for the nonlinear equations and so in order to allow comparison with existing results we shall follow most EHL studies and use a regular rectangular mesh. The governing equations are discretized with the direction of flow in the X-direction and mesh spacings h_x and h_y in the X and Y directions, respectively. Due to symmetry, only half the domain is used in the Y-direction. Reynolds equation (1) is discretized at each nonboundary mesh point (i, j), $((i-1)h_x + X_a, (j-1)h_y + Y_a)$ where $X, Y \in [X_a, X_b] \times [Y_a, Y_b]$, using central and first order backward differencing to get

$$\epsilon_{i-(1/2),j}(P_{i-1,j} - P_{i,j}) + \epsilon_{i+(1/2),j}(P_{i+1,j} - P_{i,j}) + h_x^2 h_y^{-2}(\epsilon_{i,j-(1/2)}(P_{i,j-1} - P_{i,j}) + \epsilon_{i,j+(1/2)}(P_{i,j+1} - P_{i,j})) - h_x(\rho_{i,j}H_{i,j} - \rho_{i-1,j}H_{i-1,j}) = 0 \quad (6)$$

where, $\epsilon_{i+(1/2),j}$, $\epsilon_{i-(1/2),j}$, $\epsilon_{i,j+(1/2)}$ and $\epsilon_{i,j-(1/2)}$ $(i = 2, \ldots, m_x - 1; j = 2, \ldots, n_y - 1)$ denote the values of ϵ at the intermediate locations midway between mesh points. m_x and n_y are the maximum number of points in X and Y directions, respectively.

The discretized film thickness Eq. (4) at a point (i, j) is given by:

$$H_{i,j} = H_0 + \frac{X_i^2}{2} + \frac{Y_j^2}{2} + d_{i,j} \quad (7)$$

where H_0 is a constant and $d_{i,j}$ is the elastic deformation of the material due to the applied load. The elastic deformation of the surface is derived by dividing the pressure distribution into rectangular blocks of uniform pressure. Thus the elastic deformation, $d_{X,Y}$, at a point (X, Y) due to the uniform pressure over the rectangular area $2a2b$ is given by Venner (1991b):

$$d_{X,Y} = \frac{2P}{\pi^2}\int_{-b}^{b}\int_{-a}^{a}\frac{dX'dY'}{\sqrt{(X - X')^2 + (Y - Y')^2}}. \quad (8)$$

If the entire domain is divided into equal rectangular areas, then from Dowson and Hamrock (1976), the elastic deformation, $d_{i,j}$, at a point (i, j) due to contributions of all rectangular areas of uniform pressure is given by:

$$d_{i,j} = \frac{2}{\pi^2}\sum_{k=1}^{m_x}\sum_{l=1}^{n_y} K_{m,n}P_{k,l} \quad (9)$$

where, $m = |i - k| + 1$, $n = |j - l| + 1$, m_x and n_y are the maximum number of points in the X and Y directions, respectively. The coefficients $K_{m,n}$ are given by:

$$|X_p|\ln\left(\frac{Y_p + \sqrt{X_p^2 + Y_p^2}}{Y_q + \sqrt{X_p^2 + Y_q^2}}\right) + |Y_q|\ln\left(\frac{X_q + \sqrt{Y_q^2 + X_q^2}}{X_p + \sqrt{Y_q^2 + X_p^2}}\right) + |X_q|\ln\left(\frac{Y_q + \sqrt{X_q^2 + Y_q^2}}{Y_p + \sqrt{X_q^2 + Y_p^2}}\right) + |Y_p|\ln\left(\frac{X_p + \sqrt{Y_p^2 + X_p^2}}{X_q + \sqrt{Y_p^2 + X_q^2}}\right)$$

where

$$X_p = X_i - X_k + \frac{h_x}{2}, \; X_q = X_i - X_k - \frac{h_x}{2},$$

$$Y_p = Y_j - Y_l + \frac{h_y}{2} \quad \text{and} \quad Y_q = Y_j - Y_l - \frac{h_y}{2}.$$

One advantage of a regular mesh is that the $m_x n_y$ coefficients need only be calculated once and stored. In contrast, on an irregular mesh it is necessary to store $m_x n_y$ coefficients for each mesh point.

The force balance Eq. (5) determines the value of the integration constant H_0 and is discretized as follows:

$$h_x h_y \sum_{i=1}^{m_x}\sum_{j=1}^{n_y} P_{i,j} - \frac{2\pi}{3} = 0. \quad (10)$$

The system of Eqs. (6), (9), and (10), thus constitutes a finite difference approximation to a system of integro-differential equations for the unknown variables H_0 and $P_{i,j}$. The initial pressure distribution is given by the Hertzian pressure profile $(P = (1 - X^2 - Y^2)^{1/2}$ if $X^2 + Y^2 < 1$, otherwise $P = 0)$. The system of Eqs. (6), (9), and (10) may thus be written as a nonlinear system of N_d equations of the form

$$\underline{F}(\underline{q}) = \underline{0} \quad (11)$$

where the vector of unknowns, $\underline{q}$, is defined by

$$[\underline{q}]_k = P_{i,j},\ k = (i-2)*(m_x - 2) + j - 1,$$

$$i = 2, \ldots, m_x - 1,\ j = 2, \ldots, n_y - 1$$

$$[\underline{q}]_{N_d} = H_0,\ N_d = (m_x - 2)*(n_y - 2) + 1$$

It should be noted from Eqs. (6), (9), and (10) that the Jacobian $\partial F/\partial q$ is dense due to the dependence of the film thickness, $H_{i,j}$, at any point on all the pressures $P_{k,l}$, as can be seen from Eq. (9).

Nomenclature

b = radius of Hertzian contact
G = dimensionless materials parameter
H = dimensionless film thickness
H_0 = reference datum for elastic deflections
h_x, h_y = dimensionless mesh size
L = dimensionless materials parameter (Moes)
M = dimensionless load parameter (Moes)
P = dimensionless pressure
p_h = maximum Hertzian pressure
R = reduced radius of curvature
U = dimensionless speed parameter
W = dimensionless load parameter
X_a = dimensionless inlet boundary
X_b = dimensionless outlet boundary
x, x' = coordinate
X, X' = dimensionless coordinate
Y_a, Y_b = dimensionless boundary domain
Y, Y' = dimensionless coordinate
y, y' = coordinate
z = viscosity parameter (Roelands)
α = pressure viscosity index
ϵ = coefficient in Reynolds equation
λ = dimensionless speed parameter
η = viscosity
ρ = density

Sub-, Superscripts

a, b = inlet, outlet
i, j = grid index
k, l = grid index
x, y = x, y direction

3 Multigrid Method

The use of multigrid methods in solving EHL problems is relatively new. This method was introduced into the field by Lubrecht (Lubrecht et al., 1986b), who through his extensive work has made multigrid techniques important for solving EHL problems. The use of multigrids for solving EHL line and point contact problems has been described by Venner (1991b).

The concept of multigrid iteration depends on the asymptotic nature of errors associated with iterative schemes and how the schemes reduce these errors. Smooth error components associated with low frequencies are hardly reduced with the classical iterative schemes, thus resulting in slow convergence. The opposite is true for error components with wavelength of the order of the mesh spacing. However, low frequency error components can be adequately represented on coarser grid. In a multilevel solver, which makes use of a series of coarser grids, each error component is reduced until it becomes smooth when the same procedure is applied on a coarser grid.

EHL problems are nonlinear. Thus, when using multigrids, the standard Correction Scheme cannot be used and the Full Approximation Scheme must be used instead. In the cavitation region, in which negative pressures are computed by the solver, the Reynolds equation is not valid and the computed pressures are set to zero in the standard manner as shown by Venner (1991b). This is treated with the multigrid method by using injection near and in the cavitational region when transferring the residual and the solution to the coarse grid. Full weighting is used in the remaining parts of the domain.

The FDMG Multigrid Software of Shaw (Shaw) is used here as a starting point for implementing the multigrid technique. FDMG employs Multigrid Full Approximation Scheme (FAS) to solve nonlinear systems of partial differential equations using either V or W coarse grid correction cycles. The Jacobi or Gauss Seidel iterative method can be used as a smoother. The option for the type of restriction is either injection or full weighting (Lubrecht et al., 1987a). The FDMG multigrid software is modified in order to take the cavitation condition into consideration and the Full Multigrid Scheme, Venner (1991b), is also introduced. The full multigrid scheme is also known as nested iteration and it works on the principle that coarser grids are used to generate an accurate initial approximation on the finest grid.

The solution for the isothermal point contact problem is obtained by making use of strong coupling in the direction of flow, the X-direction. This is known as I-Line relaxation, see Wesseling (1992) for more details. Thus the discrete equations are solved simultaneously on a line of points, sweeping across the grid only in the positive Y-direction due to symmetry. On each line of points, the relaxation scheme of Nurgat and Berzins (1996) is employed, as described in the next section.

4 New Relaxation Scheme

The new relaxation scheme employs the same general philosophy as used by Lubrecht and Venner in that either Gauss-Seidel or Jacobi Line relaxation schemes are used in the different regions of the computational domain. The choice of the relaxation scheme depends very much on the value of ϵ of the Reynolds equation (1). Gauss-Seidel and Jacobi Line relaxation schemes are respectively employed in the non-contact and contact regions of the computational domain. The new relaxation scheme is employed in the following manner:

Having obtained the correction terms, $\Delta \bar{P}$, using I-Line relaxation on the line $Y = j$ and before applying I-Line relaxation on the line $Y = j + 1$, at every point on the line $Y = j$ which lies in the noncontact region, as shown in Fig. 1, a new approximation $\bar{P}_{i,j}$ to $\bar{P}_{i,j}$ is computed using the equation

$$\bar{P}_{i,j} = \bar{P}_{i,j} - W\Delta P_{i,j} \qquad (12)$$

where W is the damping factor which lies in the range 0.4 to 0.9. A correct choice of W is critical to ensure convergence of the method. Besides this, all the correction terms $\Delta \bar{P}$ in the contact region on the line $Y = j$ are saved in order to update the solution in the contact region after a complete sweep.

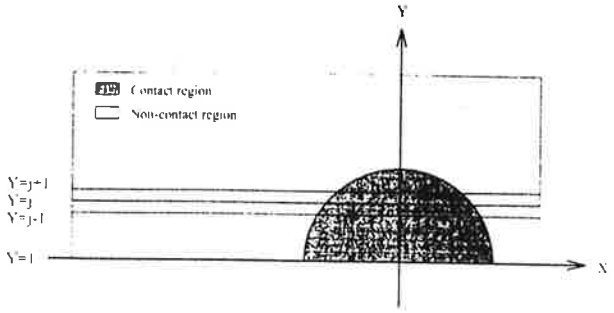

Fig. 1 Representation of contact and noncontact regions

After all interior lines j have been visited, that is after a complete sweep, a new approximation $\bar{P}_{i,j}$ to $\bar{P}_{i,j}$ is computed at every point on the entire grid which lies only in the contact region using Eq. (12) but this time the damping factor W lies in the range 0.1 to 0.2. Thus the saved values of the corrections $\Delta \bar{P}$ for the portions of each of the lines in the contact region, shown as shaded region in Fig. 1, are added en-masse at the end of the iteration. This corresponds to a block Jacobi method and is one of the distinguishing features of the scheme from that of Venner (1991b) who uses the distributive Jacobi relaxation scheme. Having updated all the pressure values on the entire grid, the elastic deformation at every point on the entire grid is recalculated using the new pressure values.

5 Homotopy Method

The concept of a homotopy is simple. It is the deformation of one problem into another by the continuous variation of a single parameter. This parameter may be part of the problem specification and therefore have some physical significance, or it may be artificial. The key point here is that one of the problems will be easy to solve, and this will be continuously deformed into one that is hard to solve. In practice, the deformation process must be discretized and a sequence of intermediate problems solved. However, by allowing the changes to be sufficiently small at each stage, it can always be arranged that the solution of one intermediate problem will lie within the domain of convergence of some locally convergent algorithm for the next. In this way, solving a series of locally convergent problems can provide a route to global convergence. This process is termed continuation (Allgower, 1990).

Consider the problem of finding a root $\underline{q}^*$ of the nonlinear equation system given by Eq. (11). A homotopy function $\underline{S}(\underline{q}, \beta)$ is a function for which $\beta \in [0, 1]$ such that the following conditions hold:

$$\underline{S}(\underline{q}, 0) = \underline{Q}(\underline{q}) \quad \text{and} \quad \underline{S}(\underline{q}, 1) = \underline{F}(\underline{q}). \qquad (13)$$

The function $\underline{S}(\underline{q}, \beta)$ (assumed to be continuous though not necessarily differentiable with respect to β) represents a continuous deformation of $\underline{Q}(\underline{q})$ into $\underline{F}(\underline{q})$ as β varies (not necessarily monotonically) from 0 to 1. If the problem of finding $\underline{q}_0$ satisfying

$$\underline{Q}(\underline{q}_0) = \underline{S}(\underline{q}_0, 0) = \underline{0} \qquad (14)$$

is one that can be solved, and a continuous solution path exists connecting $(\underline{q}_0, 0)$ to $(\underline{q}^*, 1)$ along which $\underline{S}(\underline{q}, \beta) = \underline{0}$, then continuously tracking the solution path is a globally convergent method for solving the system (11) (Allgower, 1990).

Artificially parametrized homotopy functions can be constructed in many ways, but those most usually encountered are convex linear homotopies of the form

$$\underline{S}(\underline{q}, \beta) = \beta \underline{F}(\underline{q}) + (1 - \beta)\underline{Q}(\underline{q}) \quad (15)$$

such as the fixed point homotopy

$$\underline{S}_f(\underline{q}, \beta) = \beta \underline{F}(\underline{q}) + (1 - \beta)(\underline{q} - \underline{q}_0) \quad (16)$$

where $\underline{q}_0$ can be viewed as an initial estimate of $\underline{q}^*$.

Consider the problem of finding a root of

$$\underline{S}(\underline{q}, \beta) = \underline{0} \quad (17)$$

for $\beta = 1$, where $\underline{q}$ represents the basic independent variables of the problem and one or more parameters a_i are defined in terms of β by (usually linear) relationships of the form $a_i = \varphi_i(\beta)$. The problem is assumed to have been easily solved for the root $\underline{q}_0$ corresponding to $\beta = 0$ (e.g. using a Newton-type method). The parametrized problem form is in the homotopy form but the dependence upon β is no longer necessarily linear.

We have found that an efficient homotopy technique for the robust, simultaneous solution of EHL point contact equations is the one based upon physical parametrisation, using the pressure coefficient of viscosity α as the underlying parameter:

$$\alpha = \alpha_0 + \beta(\alpha^* - \alpha_0) \quad (18)$$

when $\beta = 0$, $\alpha = \alpha_0$ (typically 5×10^{-9}, representing a near isoviscous case) and when $\beta = 1$, $\alpha = \alpha^*$ (the desired value for the oil in question is typically 2×10^{-8} or more). Nondimensionalization of the governing equations is carried out once and for all using the final value of p_h which is computed from the final value of α. Viscosity and density are computed from the local continuation values of alpha and p_h. This enables the continuation process to be carried out without changing the size of the domain, but the intermediate problems do not correspond obviously to meaningful physical problems. The initial problem is easy to solve using a Newton-type method, and working with α has the added advantage that the same mesh can be used throughout (the computational domain size does not have to change as it would were load used as a parameter, for example).

The kinds of numerical algorithm that can be used to solve this problem are surveyed in the references (Allgower, 1990). We have used a predictor-corrector algorithm. Briefly, points satisfying Eq. (17) map out a curve in $(\underline{q}, \beta)$-space, the zero curve, as β varies. The algorithm starts from one point on this curve and takes a predictor step along the tangent there. The step size is adaptive, and the algorithm tries to maintain it as large as possible. The step direction is also chosen to make doubling back along the path impossible. A series of corrector steps is then taken with the intention of converging to a point further along the zero curve. Failing that, a new predictor with a reduced step size is undertaken. A purely locally convergent projected Newton method is used for the corrector steps. It should be noted that the Jacobian matrix is full and so a dense linear equation solver is used. To save on Jacobian evaluations, the Jacobian is only updated at points on the zero curve. In practice, the zero curve does not have to be tracked with high accuracy, since accumulation of discretisation errors such as occurs, for example, in the integration of ODE systems, does not arise here (Allgower, 1990). This algorithm allows the tracking of zero curves with rapid changes of arc length and non-monotonicity with respect to β. Such situations cause the failure of simple continuation techniques where the β. Such situations cause the failure of simple continuation techniques where the β values are explicitly prescribed and monotonic.

For methods such as that just outlined, cavitation is often perceived as difficult to handle because it is not possible to arbitrarily set components of the pressure to zero without compromising convergence by introducing discontinuities. We have used penalty functions (Wu, 1986) to resolve the cavitation problem. The basic idea is to add on to the discrete Reynolds equation a term

$$\psi(P) = \gamma P^2 \quad (19)$$

for some positive constant γ, wherever the pressure is negative. In this way, the equation cannot be satisfied unless negative pressures are driven toward zero (squaring the pressure keeps the problem continuous in first derivatives). The larger γ is, the more this will be case, but also the more sudden will be changes in curvature of the problem functions. For this reason we achieve greater robustness by deriving γ continually from the homotopy parameter according to

$$\gamma = \beta\gamma^* \quad (20)$$

where γ^* is the target value (typically 1000). In order to be able to cater for the very hardest problems, we sometimes carry out the γ continuation as a separate phase following completion of the α continuation. For many problems, though, the two can be merged quite satisfactorily.

6 Test Problem One

This test problem, which appears in Wang (1994), is solved on a domain $\{(X, Y) : -4.5 \le X \le 1.2, -3.0 \le Y \le 3.0\}$ using the new relaxation scheme on a single grid and multigrid and using the homotopy method on a single grid. A 65 by 65 grid is employed when the problem is solved on a single grid using the new relaxation scheme and the homotopy method. A finest 65 by 65 grid and a coarsest 17 by 17 grid are used when the problem is solved using the multigrid method. However, due to symmetry, only the nodes in the positive Y-direction are used when the problem is solved using the new relaxation scheme on a single grid and multigrid. For this highly loaded problem, the values of Moes dimensionless parameters are $M = 99$ and $L = 16$. This in turn gives $\lambda = 2.3975 \times 10^{-2}$. The

Table 1 Test Problem One solved on a *S*-Grid, $M = 99$ and $L = 16$

Its	Hcent	Hmin	RMSRES	SumP	δP
100	0.1855	0.0967	5.6671E-03	1.9249	3.012E-03
300	0.1918	0.1023	2.4784E-04	2.0944	1.909E-06
500	0.1919	0.1023	7.2650E-06	2.0944	1.066E-07
600	0.1919	0.1023	1.2278E-06	2.0943	1.829E-08
613	0.1919	0.1023	9.9189E-07	2.0943	1.452E-08

Table 2 Test Problem One solved using *M*-Grid, $M = 99$ and $L = 16$

Its	Hcent	Hmin	RMSRES	SumP	ΔP
1	0.1950	0.1110	3.9001E-04	2.0832	2.091E-02
5	0.1928	0.1040	1.7222E-04	2.1144	2.884E-03
10	0.1927	0.1038	1.1407E-04	2.1196	2.693E-03
15	0.1927	0.1038	9.5991E-05	2.1201	2.630E-03
20	0.1927	0.1038	9.1076E-05	2.1202	2.621E-03

Table 3 Test Problem One solved using homotopy method, $M = 99$ and $L = 16$

Its	Hcent	Hmin	RMSRES	SumP	δP	alpha
1	0.6611	0.6608	1.059E-01	2.0944	1.000E+00	5.000E-09
10	0.0897	0.0489	1.289E-03	2.0944	3.202E-06	5.000E-09
11	0.0956	0.0515	1.253E-03	2.0944	8.196E-03	5.000E-09
16	0.1383	0.0740	9.280E-04	2.0944	2.284E-02	1.141E-08
36	0.2030	0.1261	6.584E-05	2.0944	1.135E-02	2.528E-08
39	0.2071	0.1296	6.817E-08	2.0944	5.809E-04	2.205E-08
40	0.2070	0.1296	2.484E-09	2.0944	4.077E-06	2.206E-08
41	0.2042	0.1271	4.769E-05	2.0944	2.632E-03	2.206E-08
42	0.2071	0.1298	2.722E-09	2.0944	3.481E-03	2.206E-08
47	0.2071	0.1304	5.851E-09	2.0944	1.150E-03	2.206E-08
48	0.2071	0.1304	3.402E-12	2.0944	2.441E-06	2.206E-08

Table 4 Summary of H cent and H min of Test Problem One, M = 99 and L = 16

Method	Hcent	Hmin	Mesh	X-domain	Y-domain
S-Grid	0.192	0.102	65 × 65	[-4.5,1.2]	[-3.0,3.0]
M-Grid	0.193	0.104	65 × 65	[-4.5,1.2]	[-3.0,3.0]
Homotopy	0.207	0.130	65 × 65	[-4.5,1.2]	[-3.0,3.0]
Wang	0.175	0.097	151 × 81	[-3.5,1.5]	[-2.0,2.0]

maximum Hertzian pressure, p_h, at this load is 1.21 GPa if $\alpha = 2.2056 \times 10^{-8}$. Hence, the value of $\bar{\alpha} = \alpha \times p_h = 27$. The equivalent Hamrock and Dowson's (1976b) dimensionless parameters with U fixed at 5.6102×10^{-11} are $W = 3.4125 \times 10^{-6}$ and $G = 4865$ assuming that both contacts are steel.

6.1 Convergence Criteria. Tables 1, 2, and 3 show how the numerical solution changes with the number of iterations. If the convergence criterion is based on the change in the pressure solution from one iteration to the next on a single grid, which is a common though perhaps unwise practice and is labeled δP in Tables 1 and 3, then the solutions obtained using the new relaxation scheme and the homotopy method on single grid have converged to the order of 10^{-8} and 10^{-6}, respectively. A more commonly used form for checking the accuracy when using the multigrid method is to check the change in the pressure solution on the finest grid and the coarser grid just below it. This is labeled as ΔP in Table 2. When the iteration has converged we would expect to see no change in this value and for this value to reflect the spatial discretization error in the coarser grid. ΔP as shown in Table 2 suggests that the pressure solution obtained using the multigrid method which employs the new relaxation scheme has converged to the order of 10^{-3}.

However, if the convergence is based on the Root Mean Square Residual, labeled RMSRES, then the solutions obtained using the new relaxation scheme on a single grid and multigrid have converged to the order of 10^{-6} and 10^{-4}, respectively. This discrepancy in the RMSRES values appears to be due to the cavitation region and the nature of the Reynolds equation. In the cavitation region, Reynolds equation is not valid and problems arises when transferring residuals and corrections between grids when using the multigrid method. This is a very important issue and needs further study. The RMSRES obtained using the homotopy method on a single grid is of the order 10^{-12}.

Also shown in Tables 1, 2, and 3 are the central, labeled Hcent, and the minimum, labeled Hmin, film thicknesses obtained using the new relaxation scheme on a single grid (S-Grid) and multigrid (M-Grid) and the homotopy method on a single grid. The final values of Hcent and Hmin obtained by Wang (1994) and ourselves are summarized in Table 4. The values of Hcent and Hmin obtained by Wang (1994), who used the effective influence method, are different from those obtained using the three different numerical schemes presented in this paper mainly due to the use of different mesh domains.

7 Test Problem Two

This test problem, which appears in Venner (1991b), is solved on a domain $\{(X, Y) : -5.0 \le X \le 1.2, -3.5 \le Y \le 3.5\}$ using the new relaxation scheme on a single grid and multigrid and using the homotopy method on a single grid. A

Table 5 Test Problem Two solved on a S-Grid, M = 20 and L = 10

Its	Hcent	Hmin	RMSRES	SumP	δP
100	0.4322	0.2914	1.1204E-02	2.0594	1.311E-03
300	0.4513	0.3048	1.9066E-03	2.0979	6.537E-05
500	0.4524	0.3054	2.5793E-04	2.0947	7.447E-06
700	0.4525	0.3054	3.3917E-05	2.0944	9.621E-07
1000	0.4525	0.3055	1.6112E-06	2.0943	4.561E-08

Table 6 Test Problem Two solved using M-Grid, M = 20 and L = 10

Its	Hcent	Hmin	RMSRES	SumP	ΔP
1	0.4612	0.3076	1.3773E-02	2.0842	1.377E-02
5	0.4529	0.3057	1.6256E-04	2.0909	8.322E-04
10	0.4526	0.3054	7.3911E-05	2.0904	2.452E-04
15	0.4525	0.3053	4.3010E-05	2.0905	2.251E-04
20	0.4525	0.3053	3.6674E-05	2.0905	2.236E-04
25	0.4525	0.3053	3.6051E-05	2.0905	2.234E-04

65 by 65 grid is employed when the problem is solved on a single grid using the new relaxation scheme and the homotopy method. A finest 65 by 65 grid and a coarsest 17 by 17 grid are used when the problem is solved using the multigrid method. However, due to symmetry, only the nodes in the positive Y-direction are used when the problem is solved using the new relaxation scheme on a single grid and multigrid. For this moderately loaded problem, the values of Moes dimensionless parameters are $M = 20$ and $L = 10$. This in turn gives $\lambda = 0.2022$. The maximum Hertzian pressure, p_h, at this load is 0.5818 GPa if $\alpha = 1.7 \times 10^{-8}$. Hence, the value of $\bar{\alpha} = \alpha \times p_h = 10$. The equivalent Hamrock and Dowson's dimensionless parameters with U fixed at 1.0×10^{-11} are $W = 1.8915 \times 10^{-7}$ and $G = 4729$ assuming that the boundary materials are different from those of Test Problem One.

7.1 Results. The numerical solutions and the convergence histories associated with the three methods are shown in Tables 5, 6, and 7. The Root Mean Square Residual, labeled RMSRES, obtained using the new relaxation scheme on a single grid and multigrid and the homotopy method are of the order 10^{-6}, 10^{-5} and 10^{-11}, respectively. Convergence based on δP when using a single grid method and ΔP when using the multigrid method, which is a general practice, suggest that the solution obtained using the new relaxation scheme on a single grid is of the order 10^{-8} as can be seen from Table 5. It is much smaller than that obtained using the other two methods which are of the order 10^{-4} and 10^{-6} as can be seen from Tables 6 and 7.

Also shown in Tables 5, 6, and 7 are the central, labeled Hcent, and the minimum, labeled Hmin, film thicknesses obtained using the new relaxation scheme on a single grid (S-Grid) and multigrid (M-Grid) and the homotopy method on a single grid. The final values of Hcent and Hmin obtained by ourselves, Venner (1991b) and Ehret (1997) are summarized in Table 8. On a 65 × 65 domain, the discrepancy between the values of Hcent and Hmin obtained using the three different numerical schemes presented in this paper is minimal. However, these values differ from those obtained by Venner (1991b). The reason for this is not clear but we have noted that slight differences in the schemes, for example using either a first or a second order upwinding, can give rise to significant differences in the results. Table 8 also shows the results obtained using the multigrid (M-Grid) method, which uses the new relaxation scheme, compared with the results of Venner (1991b)

Table 7 Test Problem Two solved using homotopy method, M = 20 and L = 10

Its	Hcent	Hmin	RMSRES	SumP	δP	alpha
1	0.6478	0.6468	4.302E-01	2.0944	1.0000E+00	5.000E-09
7	0.2466	0.1765	1.371E-02	2.0944	4.9562E-05	5.000E-09
8	0.2468	0.1765	1.369E-02	2.0944	2.3835E-04	5.000E-09
14	0.3600	0.2440	8.178E-03	2.0944	5.6744E-02	1.096E-08
20	0.4411	0.2953	2.023E-03	2.0944	3.8711E-03	1.773E-08
23	0.4477	0.2998	1.349E-03	2.0944	4.5581E-03	1.652E-08
24	0.4372	0.2927	2.333E-03	2.0944	1.7103E-02	1.576E-08
31	0.4530	0.3034	7.721E-04	2.0944	7.2105E-03	1.733E-08
37	0.4604	0.3086	2.533E-07	2.0944	3.7252E-04	1.700E-08
38	0.4604	0.3086	9.132E-09	2.0944	2.9120E-06	1.700E-08
44	0.4605	0.3130	1.282E-07	2.0944	2.7799E-03	1.700E-08
45	0.4605	0.3130	2.762E-11	2.0944	3.3570E-06	1.700E-08

Table 8 Summary of H cent and H min of Test Problem Two, M = 20 and L = 10

Method	Hcent	Hmin	Mesh	X-domain	Y-domain
S-Grid	0.453	0.306	65 × 65	[-5,1.2]	[-3.5,3.5]
M-Grid	0.453	0.305	65 × 65	[-5,1.2]	[-3.5,3.5]
Homotopy	0.460	0.313	65 × 65	[-5,1.2]	[-3.5,3.5]
Venner	0.489	0.355	65 × 65	[-4.5,1.5]	[-3.0,3.0]
M-Grid	0.443	0.304	257 × 257	[-4.5,1.5]	[-3.0,3.0]
Venner	0.498	0.345	257 × 257	[-4.5,1.5]	[-3.0,3.0]
Ehret	0.431	0.295	257 × 257	[-4.5,1.5]	[-3.0,3.0]

and Ehret, who communicated his results to us, on different mesh sizes and domains. A summary of these results is that the results obtained using the three different numerical schemes presented in this paper and by Ehret are relatively close while the results of Venner are some what more distant, though still comparable.

7.2 Remarks. A point to note is that, when using the homotopy method, the force balance equation, labeled SumP in Tables 3 and 7, is satisfied on every iteration but this is not the case when the new relaxation scheme is employed on a single grid or multigrid.

An interesting feature about homotopy method is the sudden sharp drop in RMSRES as can be seen more clearly from Table 7. This may be attributed to the quadratic rate of convergence of the homotopy method close to the root. A sharp decrease in δP can also be noticed in Tables 3 and 7.

Since Homotopy method is very expensive in terms of computational time, it was not possible to use a finer mesh than 65 by 65. For the two test problems, the times taken to achieve the results using the new relaxation scheme on a single grid and multigrid and the homotopy method were 8.25 mins, 3.2 mins, and 6.06 hr, respectively, for test problem one and for test problem two the times were 13.5 mins, 2.9 mins, and 5.73 hr, respectively. An SGI R8000 was used for the first two numerical methods and an R10000 processor for the homotopy method.

8 Discussion and Conclusions

From the results obtained we can say something about the efficiency of the new relaxation scheme employed on a single grid and multigrid. The accuracy obtained when the new relaxation scheme is used on a single grid suggest the efficiency of this very simple relaxation scheme. This new relaxation scheme is explained in detail and compared with the distributive relaxation scheme of Venner (1991b) in Nurgat and Berzins (1996). The numerical results shown in this paper demonstrate how even a relatively standard multigrid code when used with the new relaxation scheme may be used to speed up the solution of EHL problems. However, this speed can be further enhanced by making use of the multi-integration scheme (Brandt and Venner, 1990) to compute the elastic deformation. The homotopy method has the property of being very robust and has the additional advantage of delivering better convergence in terms of the residual but this is at the expense of much longer CPU times. There is, however, considerable scope for reducing these CPU times by using iterative methods for the linear equation solution rather than the Gaussian elimination methods employed here. This is an area of our current research (Schlijper et al., 1996).

The numerical results shown above raise an outstanding issue concerning the treatment of convergence in EHL problems. A further issue, that is of concern, appears to be the effect of domain size on the final results.

Acknowledgments

The authors would like to thank EPSRC and Shell Research Ltd, Thornton Research Centre for funding this work through an EPSRC CASE Studentship for E.N. Our colleagues at Leeds in the Mechanical Engineering Department D. Dowson, C. Taylor, and P. Ehret are thanked for providing much constructive advice and support. Gareth Shaw of NAG Ltd is thanked for supplying the FDMG code.

References

Allgower, E. L., and Georg, K., 1990, *Numerical Continuation Methods*, Springer-Verlag.

Brandt, A., and Lubrecht, A. A., 1990, "Multilevel Matrix Multiplication and Fast Solution of Integral Equations," *Journal of Computational Physics*, No. 2, pp. 348–370.

Dowson, D., and Higginson, G. P., 1977, *Elastohydrodynamic Lubrication*, Pergamon Press.

Dowson, D., and Hamrock, B. J., 1976, "Numerical Evaluation of the Surface Deformation of Elastic Solids Subjected to a Hertzian Contact Stress," *ASLE Trans.*, Vol. 19, No. 4, pp. 279–286.

Ehret, P., Dowson, D., Taylor, C. M., and Wang, D., "Analysis of EHL Point Contacts with Multigrid Methods," To be published in *IMECHE*, Part C.

Garcia, C. B., and Zangwill, W. I., 1981, *Pathways to Solutions, Fixed Points and Equilibria*, Prentice-Hall.

Gohar, R., 1988, *Elastohydrodynamics*, Ellis Horwood Limited, Chichester, England.

Hamrock, B. J., and Dowson, D., 1977, "Isothermal Elastohydrodynamic Lubrication of Point Contacts, Part III, Fully Flooded Results," ASME JOURNAL OF LUBRICATION TECHNOLOGY, Vol. 99, pp. 264–276.

Hamrock, B. J., and Dowson, D., 1976, "Isothermal Elastohydrodynamic Lubrication of Point Contacts, Part I, Theoretical Formulation," ASME JOURNAL OF LUBRICATION TECHNOLOGY, Vol. 98, pp. 223–229.

Lubrecht, A. A., ten Napel, W. E., and Bosnia, R., 1987, "Multigrid—An Alternative Method of Solution for Two-dimensional Elastohydrodynamically Lubricated Point Contact Calculations," ASME JOURNAL OF TRIBOLOGY, Vol. 109, pp. 437–443.

Lubrecht, A. A., ten Napel, W. E., and Bosma, R., 1986, "Multigrid—An Alternative Method of Calculating Film Thickness and Pressure Profiles in Elastohydrodynamically Lubricated Line Contacts," ASME JOURNAL OF TRIBOLOGY, Vol. 108, No. 4, pp. 551–556.

Nurgat, E., and Berzins, M., 1996, "A New Relaxation Scheme for Solving EHL Problems," To be published in the *23rd Leeds-Lyon Symposium on Tribology*.

Roelands, C. J. A., 1966, "Correlational Aspects of the Viscosity-Temperature-Pressure Relationship of Lubricating Oils," Ph.D thesis, Technische Hogeschool Delft, The Netherlands.

Schlijper, A. G., Scales, L. E., and Rycroft, J. E., 1996, "Current Tools and Techniques for EHL Modelling," *Tribology International*, Vol. 29, pp. 669–673.

Shaw, G. J., *FDMG Multigrid Software Manual*, version 3.0.

Venner, C. H., 1994, "Higher-Order Multilevel Solvers for the EHL Line and Point Contact Problem," ASME JOURNAL OF TRIBOLOGY, Vol. 116, Oct., pp. 741–750.

Venner, C. H., and Lubrecht, A. A., 1994, "Numerical Simulation of a Transverse Ridge in a Circular EHL Contact Under Rolling/Sliding," ASME JOURNAL OF TRIBOLOGY, Vol. 116, Oct., pp. 751–761.

Venner, C. H., 1991, "Multilevel Solution of the EHL Line and Point Contact Problems," Ph.D. thesis, University of Twente, The Netherlands, ISBN 90-9003974-0.

Wang, D., 1994, "Elastohydrodynamic Lubrication of Point Contacts for Layers of 'Soft' Solids and for 'Monolithic' 'Hard' Materials in the Transient Bouncing Ball Problems," Ph.D. thesis, Department of Mechanical Engineering, University of Leeds.

Wesseling, P., 1992, *An Introduction to Multigrid Methods*, Wiley, Chichester, England.

Wu S. R., 1986, "A Penalty Formulation and Numerical Approximation of the Reynolds-Hertz Problem of Elastohydrodynamic Lubrication," *J. Engng. Sci.*, Vol. 24, pp. 1001–1013.